

文章编号: 1001-3806(2020)03-0338-05

厄米-高斯波束对各向异性圆柱的散射特性研究

查晓民¹, 朱东²

(1. 铜陵学院 数学与计算机学院, 铜陵 244000; 2. 安徽大学 电子信息工程学院, 合肥 230039)

摘要: 为了研究厄米-高斯波束在各向异性媒质中的散射特性, 采用了将各向异性圆柱的散射场和内部场用圆柱矢量波函数展开, 应用电磁场边界条件和投影法, 提出了一种分析单轴各向异性圆柱对厄米-高斯波束散射特性研究的精确半解析方法; 获得了厄米-高斯波束通过单轴各向异性圆柱的内场以及近场的归一化强度分布图; 对两种不同的厄米-高斯波束入射情形做出了分析和对比。结果表明, 两种波束在通过圆柱后都有入射波和反射波叠加而成的驻波现象, 而 $TEM_{10}^{(x)}$ 模式厄米-高斯波束入射后近场强度增强, 且有明显的折射现象。该研究结果对厄米-高斯波束的应用具有一定的参考价值。

关键词: 散射; 厄米-高斯波束; 圆柱矢量波函数; 边界条件; 投影法

中图分类号: TN012; O436.2 **文献标志码:** A **doi:** 10.7510/jgjs.issn.1001-3806.2020.03.012

Scattering characteristics of Hermite-Gaussian beam on anisotropic cylinder

ZHA Xiaomin¹, ZHU Dong²

(1. School of Mathematics and Computer, Tongling University, Tongling 244000, China; 2. School of Electronic Information Engineering, Anhui University, Hefei 230039, China)

Abstract: In order to research the scattering properties of Hermite-Gaussian beams in anisotropic media, the paper used a cylindrical vector wave function for the scattering field and internal field of an anisotropic cylinder. Using electromagnetic field boundary conditions and projection method, a method was proposed. The accurate semi-analytical method for studying the scattering properties of Hermite-Gaussian beams from uniaxial anisotropic cylinders was analyzed. The normalized intensity distributions of both the internal-field and near fields of the Hermitian-Gaussian beams through an uniaxial anisotropic cylinder were obtained. The analysis and comparison of two different Hermitage beam incidents were carried out. The results show that both beams have a standing wave phenomenon caused by the superposition of incident and reflected waves after passing through the cylinder, while the $TEM_{10}^{(x)}$ mode Hermite-Gaussian beam has a enhanced near-field intensity and a significant refraction phenomenon after its incidence. The research results have certain reference value for the application of Hermite-Gaussian beam.

Key words: scattering; Hermite-Gaussian beam; cylindrical vector wave functions; boundary conditions; projection method

引言

近些年来, 高斯波束在各向异性材料中传播特性一直受到持续性的关注, 该研究不仅具有重要的理论价值, 而且一些成果已广泛应用于雷达散射截面、光信号处理、微波器件、天线罩、光纤的优化设计和微带天线等领域。1972年, ALEXOPOULOS等人^[1]研究了无限长非均匀介质圆柱对高斯波束片的散射。LOCK^[2]研究了无限长均匀圆柱体对入射聚焦高斯光束的散射

问题。GUO等人^[3]提出一种有效而精确的递推算法来计算高斯波束垂直入射无限长多层圆柱的散射问题, 并重点分析了圆柱的彩虹效应。随着广义洛伦兹-米理论的发展, HUANG和ZHANG等人^[4-6]通过将圆柱散射场、内场和入射的高斯光束用适当的圆柱矢量波函数展开, 应用电磁场边界条件, 解析地解决了高斯光束在单轴各向异性圆柱体上的散射特性。CHEN和ZHANG等人^[7]提出一种精确的半解析方法来计算回旋各向异性圆柱体对在轴高斯光束的散射问题。高斯波束的研究及其性质已经非常成熟^[8-14], 只有少量文献中研究了其它高斯波束的性质^[15-18]。

厄米-高斯波束是由高斯波束演化而来, 具有重要的理论价值。作者在前人基础上, 重点研究了厄米-高斯波束, 首先讨论了电磁媒质的本构关系和分类, 其次

作者简介: 查晓民(1980-), 男, 硕士, 讲师, 主要从事计算电磁学方面的研究。

E-mail: sunnyrain1115@126.com

收稿日期: 2019-05-08; 收到修改稿日期: 2019-06-13

讨论了厄米-高斯波束在单轴各向异性圆柱中的散射特性,最后给出了数值结果和结论。

1 电磁媒质的本构关系和分类

任意电磁媒质的本构关系可表达为:

$$\begin{cases} \mathbf{D} = \overline{\overline{\boldsymbol{\varepsilon}}} \cdot \mathbf{E} + \overline{\overline{\boldsymbol{\xi}}} \cdot \mathbf{H} \\ \mathbf{B} = \overline{\overline{\boldsymbol{\mu}}} \cdot \mathbf{H} + \overline{\overline{\boldsymbol{\zeta}}} \cdot \mathbf{E} \end{cases} \quad (1)$$

式中, \mathbf{D} 是电位移, \mathbf{E} 是电场强度, \mathbf{B} 是磁感应强度, \mathbf{H} 是磁场强度, $\overline{\overline{\boldsymbol{\xi}}}$ 和 $\overline{\overline{\boldsymbol{\zeta}}}$ 为手征参量张量, $\overline{\overline{\boldsymbol{\varepsilon}}}$ 和 $\overline{\overline{\boldsymbol{\mu}}}$ 分别为媒质的介电常数张量和磁导率张量。当媒质的磁导率为标量, 介电常数为张量时, 称媒质为电各向异性媒质, 反之为磁各向异性媒质。在直角坐标系 $Oxyz$ 中, 电各向异性媒质中的介电常数可表示为 $\overline{\overline{\boldsymbol{\varepsilon}}} = \hat{x}\hat{x}\varepsilon_1 + \hat{y}\hat{y}\varepsilon_2 + \hat{z}\hat{z}\varepsilon_3$, 而 \mathbf{D} 与 \mathbf{E} 的关系可表示为:

$$\begin{bmatrix} D_x \\ D_y \\ D_z \end{bmatrix} = \begin{bmatrix} \varepsilon_1 & 0 & 0 \\ 0 & \varepsilon_2 & 0 \\ 0 & 0 & \varepsilon_3 \end{bmatrix} \begin{bmatrix} E_x \\ E_y \\ E_z \end{bmatrix} \quad (2)$$

式中, 下标 x, y, z 表示电场的 3 个方向分量; $\hat{x}, \hat{y}, \hat{z}$ 为电场的 3 个方向的单位矢量。若 $\varepsilon_1, \varepsilon_2, \varepsilon_3$ 全部相等, 称为各向同性媒质; 若其中有两个相等, 称为单轴各向异性媒质; 若 3 个对角元素均不相等, 则称为双轴各向异性媒质。本文中主要研究单轴各向异性媒质 $\varepsilon_1 = \varepsilon_2$ 的情形。

2 厄米-高斯波束在单轴各向异性圆柱中的散射特性

2.1 散射场和圆柱内场用圆柱矢量波函数展开

如图 1 所示^[4], 在直角坐标系 $Oxyz$ 中有一个半径为 r_0 的无限长单轴各向异性圆柱体, 高斯波束在自由空间且沿直角坐标系 $Ox'y'z'$ 的 z' 轴正方向传播, 高斯波束的束腰半径为 w_0 , 束腰中心与圆心 O' 重合。波束的传播方向与 z 轴正方向夹角为 β , 在 $O'x'y'z'$ 中点

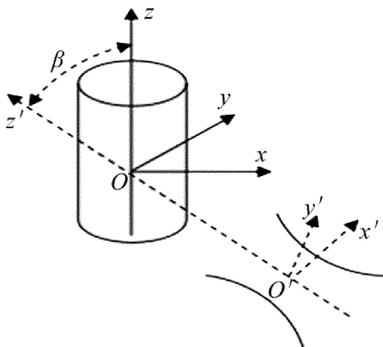


Fig. 1 The incidence of a Gaussian beam on an uniaxial anisotropic cylinder

O 坐标为 (x_0, y_0, z_0) 。随时间变化的部分规定为 $\exp(-i\omega t)$ 。

正如参考文献[4]中所描述的, 散射场用圆柱矢量波函数展开的表达式为:

$$\mathbf{E}_s = E_0 \sum_{m=-\infty}^{\infty} \int_0^{\pi} [\alpha_m(\zeta) \mathbf{m}_{m\lambda}^{(3)} + \beta_m(\zeta) \mathbf{n}_{m\lambda}^{(3)}] e^{ihz} d\zeta \quad (3)$$

$$\mathbf{H}_s = -iE_0 \frac{1}{\eta_0} \sum_{m=-\infty}^{\infty} \int_0^{\pi} [\alpha_m(\zeta) \mathbf{n}_{m\lambda}^{(3)} + \beta_m(\zeta) \mathbf{m}_{m\lambda}^{(3)}] e^{ihz} d\zeta \quad (4)$$

同样参考文献[4]中的单轴各向异性圆柱内部电磁场表示为:

$$\mathbf{E}_w = E_0 \sum_{q=1}^2 \sum_{m=-\infty}^{\infty} \int_0^{\pi} F_{mq}(\zeta) [\alpha_{q,e}(\zeta) \mathbf{m}_{m\lambda_q}^{(1)} + \beta_{q,e}(\zeta) \mathbf{n}_{m\lambda_q}^{(1)} + \gamma_{q,e}(\zeta) \mathbf{l}_{m\lambda_q}^{(1)}] e^{ihz} d\zeta \quad (5)$$

$$\mathbf{H}_w = -iE_0 \frac{1}{\eta_0} \sum_{q=1}^2 \sum_{m=-\infty}^{\infty} \int_0^{\pi} \frac{k_q}{k_0} F_{mq}(\zeta) \times [\beta_{q,e}(\zeta) (\zeta) \mathbf{m}_{m\lambda_q}^{(1)} + \alpha_{q,e}(\zeta) \mathbf{n}_{m\lambda_q}^{(1)}] e^{ihz} d\zeta \quad (6)$$

(3)式~(6)式中, $\mathbf{E}_s, \mathbf{H}_s$ 表示散射场中电场和磁场, $\mathbf{E}_w, \mathbf{H}_w$ 表示圆柱内部的电场和磁场, $\lambda = k_0 \sin \zeta$, $h = k_0 \cos \zeta$, k_0 为自由空间中的波数, ζ 为圆柱矢量波与坐标轴 z 方向的夹角; E_0 为电场振幅, η_0 为波阻抗; $\mathbf{m}_{m\lambda_q}^{(j)}, \mathbf{n}_{m\lambda_q}^{(j)}, \mathbf{l}_{m\lambda_q}^{(j)}$ 是圆柱矢量波函数, $j=1, 2, 3$ 分别对应三类贝塞尔函数; 而 $\alpha_m(\zeta), \beta_m(\zeta), F_{m1}(\zeta)$ 和 $F_{m2}(\zeta)$ 是待求的未知系数。可以令 $a_1^2 = \omega^2 \varepsilon_1 \mu_0, a_2^2 = \omega^2 \varepsilon_3 \mu_0, \varepsilon_0$ 和 μ_0 是自由空间中的介电常数和磁导率, 则式中其它参量为: $k_1 = a_1, k_2 = [a_1^2 a_2^2 + (a_1^2 - a_2^2) k_0^2 \cos^2 \zeta]^{1/2} / a_1, \lambda_1 = \sqrt{a_1^2 - k_0^2 \cos^2 \zeta}, \lambda_2 = a_2 a_1^{-1} \sqrt{a_1^2 - k_0^2 \cos^2 \zeta}, \alpha_{1,e}(\zeta) = 1, \beta_{1,e}(\zeta) = \gamma_{1,e}(\zeta) = \alpha_{2,e}(\zeta) = 0, \beta_{2,e}(\zeta) = -i \times$

$$\frac{a_1^2 a_2}{\sqrt{(a_1^2 - k_0^2 \cos^2 \zeta) [a_1^2 a_2^2 + (a_1^2 - a_2^2) k_0^2 \cos^2 \zeta]}}, \gamma_{2,e}(\zeta) = \frac{a_1^2 - a_2^2}{a_1^2} \frac{a_1 a_2 k_0 \cos \zeta \sqrt{a_1^2 - k_0^2 \cos^2 \zeta}}{a_1^2 a_2^2 + (a_1^2 - a_2^2) k_0^2 \cos^2 \zeta}$$

2.2 未知系数的求解

电磁场的切向分量在 $r = r_0$ 的边界连续, 则边界条件可以表示为:

$$\begin{cases} \hat{r} \times (\mathbf{E}_s + \mathbf{E}_i) = \hat{r} \times \mathbf{E}_w \\ \hat{r} \times (\mathbf{H}_s + \mathbf{H}_i) = \hat{r} \times \mathbf{H}_w \end{cases}, (r = r_0) \quad (7)$$

式中, \mathbf{E}_i 和 \mathbf{H}_i 表示入射电磁波束的电场和磁场。将(3)式~(6)式代入到(7)式中, 边界条件可以写为:

$$\hat{r} \times E_0 \sum_{m=-\infty}^{\infty} \int_0^{\pi} [\alpha_m(\zeta) \mathbf{m}_{m\lambda}^{(3)} + \beta_m(\zeta) \mathbf{n}_{m\lambda}^{(3)}] \times e^{ihz} d\zeta + \hat{r} \times \mathbf{E}_i |_{r=r_0} =$$

$$\hat{r} \times E_0 \sum_{q=1}^2 \sum_{m=-\infty}^{\infty} \int_0^{\pi} F_{mq}(\zeta) [\alpha_{q,e}(\zeta) \mathbf{m}_{m\lambda_q}^{(1)} + \beta_{q,e}(\zeta) \mathbf{n}_{m\lambda_q}^{(1)} + \gamma_{q,e}(\zeta) \mathbf{l}_{m\lambda_q}^{(1)}] e^{ihz} d\zeta \quad (8)$$

$$\begin{aligned} & \hat{r} \times E_0 \sum_{m=-\infty}^{\infty} \int_0^{\pi} [\alpha_m(\zeta) n_{m\lambda}^{(3)} + \beta_m(\zeta) \mathbf{m}_{m\lambda}^{(3)}] e^{ihz} d\zeta + \hat{r} \times i\eta_0 \mathbf{H}_i |_{r=r_0} = \\ & \hat{r} \times E_0 \sum_{q=1}^2 \sum_{m=-\infty}^{\infty} \int_0^{\pi} \frac{k_q}{k_0} F_{mq}(\zeta) [\beta_{q,e}(\zeta) (\zeta) \mathbf{m}_{m\lambda_q}^{(1)} + \alpha_{q,e}(\zeta) \mathbf{n}_{m\lambda_q}^{(1)}] e^{ihz} d\zeta \quad (9) \end{aligned}$$

遵循投影法的一般理论步骤,分别在(8)式和(9)式两边点乘 $\hat{z}e^{-ih_1z}e^{-im'\varphi}$ 和 $\hat{\varphi}e^{-ih_1z}e^{-im'\varphi}$,然后在圆柱面进行积分,可以得到未知的展开系数与 \mathbf{E}_i 和 \mathbf{H}_i 的关系式:

$$\begin{aligned} & \xi \frac{d}{d\xi} H_m^{(1)}(\xi) \alpha_m(\zeta) + \frac{hm}{k_0} H_m^{(1)}(\xi) \beta_m(\zeta) - \\ & F_{m1}(\zeta) \xi_1 \frac{d}{d\xi_1} J_m(\xi_1) - F_{m2}(\zeta) \times \\ & [\beta_{2,e}(\zeta) \frac{hm}{k_2} J_m(\xi_2) - \gamma_{2,e}(\zeta) im J_m(\xi_2)] = \\ & \left(\frac{1}{2\pi}\right)^2 \frac{1}{E_0} \xi \int_{-\infty}^{\infty} dz \int_0^{2\pi} \hat{r} \times \mathbf{E}_i \cdot \\ & \hat{z} \exp(-im\varphi) \exp(-ihz) d\varphi \quad (10) \end{aligned}$$

$$\begin{aligned} & \xi^2 H_m^{(1)}(\xi) \beta_m(\zeta) - F_{m2}(\zeta) \frac{k_0}{k_2} \xi_2^2 J_m(\xi_2) \times \\ & [\beta_{2,e}(\zeta) + \gamma_{2,e}(\zeta) \frac{ihk_2}{\lambda_2^2}] = \left(\frac{1}{2\pi}\right)^2 \frac{1}{E_0} (k_0 r_0)^2 \times \\ & \sin\xi \int_{-\infty}^{\infty} dz \int_0^{2\pi} \hat{r} \times \mathbf{E}_i \cdot \\ & \hat{\varphi} \exp(-im\varphi) \exp(-ihz) d\varphi \quad (11) \end{aligned}$$

$$\begin{aligned} & \frac{hm}{k_0} H_m^{(1)}(\xi) \alpha_m(\zeta) + \xi \frac{d}{d\xi} H_m^{(1)}(\xi) \beta_m(\zeta) - \\ & \frac{hm}{k_0} F_{m1}(\zeta) J_m(\xi_1) - \end{aligned}$$

$$\begin{aligned} & \frac{k_2}{k_0} F_{m2}(\zeta) \beta_{2,e}(\zeta) \xi_2 \frac{d}{d\xi_2} J_m(\xi_2) = \\ & i\eta_0 \frac{1}{E_0} \left(\frac{1}{2\pi}\right)^2 \xi \int_{-\infty}^{\infty} dz \int_0^{2\pi} \hat{r} \times \mathbf{H}_i \cdot \hat{z} e^{-im\varphi} e^{-ihz} d\varphi \quad (12) \end{aligned}$$

$$\begin{aligned} & \xi^2 H_m^{(1)}(\xi) \alpha_m(\zeta) - F_{m1}(\zeta) \xi_1^2 J_m(\xi_1) = \\ & i\eta_0 \frac{1}{E_0} \left(\frac{1}{2\pi}\right)^2 (k_0 r_0)^2 \sin\xi \int_{-\infty}^{\infty} dz \int_0^{2\pi} \hat{r} \times \\ & \mathbf{H}_i \cdot \hat{\varphi} \exp(-im\varphi) \exp(-ihz) d\varphi \quad (13) \end{aligned}$$

式中, $\xi = \lambda r_0$, $\xi_1 = \lambda_1 r_0$ 和 $\xi_2 = \lambda_2 r_0$ 。

2.3 厄米-高斯波束

DAVIS 和 BARTON 给出了一种计算方法^[19-20],高

斯波束 $\text{TEM}_{00}^{(y')}$ 或 TE 模在坐标系 $O'x'y'z'$ 中电磁分量中各阶近似描述可表示为:

$$E_{x'} = E_0 s^2 (-2Q^2 \xi \eta) \psi_0 e^{i\zeta/s^2} \quad (14)$$

$$E_{y'} = E_0 [1 + s^2 (iQ^3 \rho^4 - Q^2 \rho^2 - 2Q^2 \eta^2)] \psi_0 e^{i\zeta/s^2} \quad (15)$$

$$E_{z'} = E_0 [2sQ\eta + s^3 (2iQ^4 \rho^4 \eta - 6Q^3 \rho^2 \eta)] \psi_0 e^{i\zeta/s^2} \quad (16)$$

$$H_{x'} = -\frac{E_0}{\eta} [1 + s^2 (iQ^3 \rho^4 - Q^2 \rho^2 - 2Q^2 \xi^2)] \psi_0 e^{i\zeta/s^2} \quad (17)$$

$$H_{y'} = \frac{E_0}{\eta} s^2 2Q^2 \xi \eta \psi_0 e^{i\zeta/s^2} \quad (18)$$

$$H_{z'} = -\frac{E_0}{\eta} [2sQ\xi + s^3 (-6Q^3 \rho^2 \xi + 2iQ^4 \rho^4 \xi)] \psi_0 e^{i\zeta/s^2} \quad (19)$$

式中, $s = 1/(kw_0)$, $\psi_0(\xi, \eta, \zeta) = iQ \exp(-i\rho^2 Q)$, $Q = 1/(i-2\zeta)$, $\rho^2 = \xi^2 + \eta^2$ 。

根据电磁场理论中的对偶关系,即在(14)式~(19)式中做如下替换: $\mathbf{E} \rightarrow -\mathbf{H}$, $\mathbf{H} \rightarrow \mathbf{E}$, $\varepsilon_0 \rightarrow \mu_0$, $\mu_0 \rightarrow \varepsilon_0$,得到的电磁场分量仍然近似满足麦克斯韦方程组,是高斯波束的 $\text{TEM}_{00}^{(x')}$ 或 TM 模。

正如参考文献[19]中提到的,厄米-高斯波束的各种模式可以通过求解 $\text{TEM}_{00}^{(y')}$ 或 $\text{TEM}_{00}^{(x')}$ 的偏导数得到,即:

$$\text{TEM}_{mn}^{(y')} = \frac{\partial^m \partial^n \text{TEM}_{00}^{(y')}}{\partial \xi^m \partial \eta^n} \quad (20)$$

$$\text{TEM}_{mn}^{(x')} = \frac{\partial^m \partial^n \text{TEM}_{00}^{(x')}}{\partial \xi^m \partial \eta^n} \quad (21)$$

式中, ξ 和 η 为无量纲的参量: $\xi = x'/w_0$, $\eta = y'/w_0$, w_0 为高斯波束束腰半径。

为了得到厄米-高斯波束的具体表达式,以 $\text{TEM}_{01}^{(y')}$ 为例,即在(20)式中令 $m=0, n=1$ 可得:

$$\text{TEM}_{01}^{(y')} = \frac{\partial \text{TEM}_{00}^{(y')}}{\partial \eta} \quad (22)$$

将(14)式~(19)式代入(22)式,即可求得 $\text{TEM}_{01}^{(y')}$ 模:

$$E_{x'} = E_0 s^2 (-2Q^2 \xi + 4iQ^3 \xi \eta^2) \psi_0 e^{i\zeta/s^2} \quad (23)$$

$$E_{y'} = E_0 \{-2iQ + s^2 [2iQ^3 (5\eta^2 + 3\xi^2) - 6Q^2 + 2Q^4 \rho^4]\} \eta \psi_0 e^{i\zeta/s^2} \quad (24)$$

$$E_{z'} = E_0 \{s(2Q - 4iQ^2 \eta^2) + s^3 [-Q^3 (18\eta^2 + 6\xi^2) + iQ^4 \rho^2 (22\eta^2 + 2\xi^2) + 4Q^5 \rho^4 \eta^2]\} \psi_0 e^{i\zeta/s^2} \quad (25)$$

$$H_{x'} = \frac{E_0}{\eta} \{2iQ + s^2 [2Q^2 - iQ^3 (10\xi^2 +$$

$$6\eta^2) - 2Q^4\rho^4] \} \eta\psi_0 e^{i\zeta/s^2} \quad (26)$$

$$H_y = \frac{E_0}{\eta} s^2 2Q^2 \xi (1 - 2iQ\eta^2) \psi_0 e^{i\zeta/s^2} \quad (27)$$

$$H_z = -\frac{E_0}{\eta} \{ s(-4iQ^2) + s^3[-12Q^3 + 20iQ^4\rho^2 + 4Q^5\rho^4] \} \xi\eta\psi_0 e^{i\zeta/s^2} \quad (28)$$

(23)式~(28)式即为厄米-高斯波束的具体表达式。类似可得出厄米-高斯波束的 $TEM_{10}^{(x')}$ 模。

图2代表的是厄米-高斯波束 $TEM_{01}^{(y')}$ 的强度分布图,图3代表的是厄米-高斯波束 $TEM_{10}^{(x')}$ 的强度分布图。图中横纵坐标 ξ, η 均是无量纲的参量。

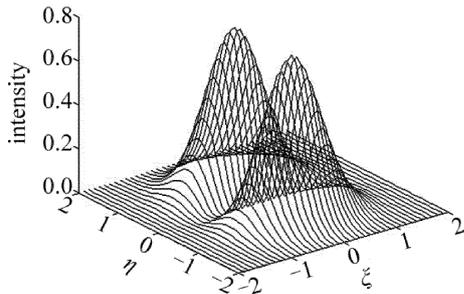


Fig. 2 The intensity distribution of the $TEM_{10}^{(y')}$ mode Hermite-Gaussian beam

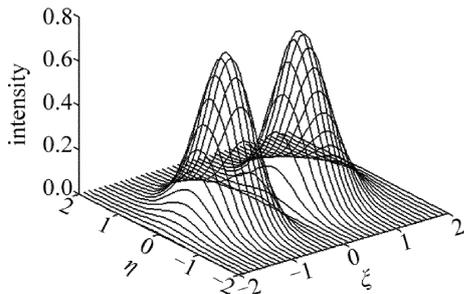


Fig. 3 The intensity distribution of the $TEM_{10}^{(x')}$ mode Hermite-Gaussian beam

2.4 数值计算结果

入射的波束,其 E_i 和 H_i 可由(23)式~(28)式得到,代入到(10)式~(13)式,可以得到未知展开系数 $\alpha_m(\zeta), \beta_m(\zeta), F_{m1}(\zeta)$ 和 $F_{m2}(\zeta)$ 构成的线性方程组,从而求出这些未知系数。求出这些系数后再代入到(3)式~(6)式,进而可以求出散射场和内场。

定义归一化内场和近场的强度分布如下:

$$|E_w/E_0|^2 = |E_{w,r}|^2 + |E_{w,\varphi}|^2 + |E_{w,z}|^2 \quad (29)$$

$$|(E_i + E_s)/E_0|^2 = |E_{i,r} + E_{s,r}|^2 + |E_{i,\varphi} + E_{s,\varphi}|^2 + |E_{i,z} + E_{s,z}|^2 \quad (30)$$

式中, $E_{w,r}, E_{w,\varphi}, E_{w,z}$ 分别为圆柱内部场中电场的3个分量; $E_{i,r}, E_{i,\varphi}, E_{i,z}$ 分别为入射场中电场的3个分量; $E_{s,r}, E_{s,\varphi}, E_{s,z}$ 分别为散射场中电场的3个分量。

对于高斯波束入射的情形,使用的参量与模型是:

单轴各向异性圆柱 $a_1 = \sqrt{3}k_0, a_2 = \sqrt{2}k_0$, 高斯波束的束腰半径 w_0 为2倍入射高斯波束的波长,圆柱的半径为5倍入射高斯波束的波长,入射角 $\beta = \pi/4, z_0 = 0$ 。图4表示高斯波束 TE 模通过单轴各向异性圆柱的归一化内场和近场。其中对于 x (wavelength) 轴上的范围, 5~15 表示入射场, -5~5 表示圆柱的内场, -15~-5 表示透射场,图中色柱表示的物理量是无量纲的。

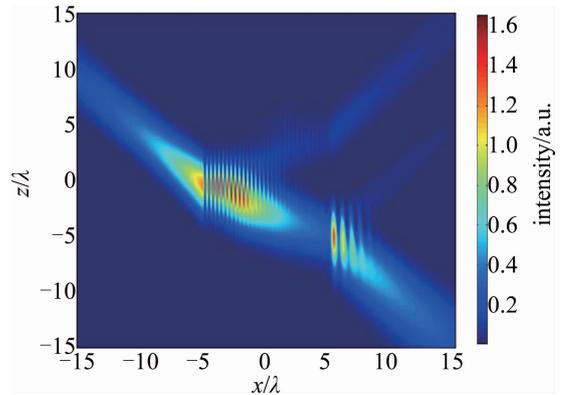


Fig. 4 The normalized internal-field and near-field of a TE mode Gaussian beam through an uniaxial anisotropic cylinder

通过与已有方法及结果^[4]比较可以发现,两者实现了很好的吻合,这在很大程度上验证了作者方法的正确性。

使用相同的参量和模型,可得厄米-高斯波束入射的情形,图5和图6分别表示厄米高斯波束 $TEM_{10}^{(x')}$ 模和 $TEM_{01}^{(y')}$ 通过单轴各向异性圆柱的归一化内场和近场。

从图5可以看出, $TEM_{10}^{(x')}$ 模式厄米-高斯波束入射单轴各向异性圆柱时的反射场强度很弱。圆柱类似于凸透镜,有一个会聚作用,所以波束在通过圆柱后的近场强度明显增强,由入射波和反射波叠加而成的驻波现象也同样在图中表现的非常明显。在图6中,波束透过圆柱后内部场强度逐渐增强,同样也有驻波现

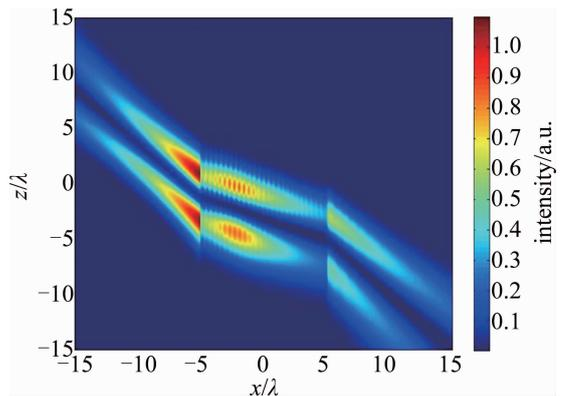


Fig. 5 The normalized internal-field and near-field of a $TEM_{10}^{(x')}$ mode Hermite-Gaussian beam through an uniaxial anisotropic cylinder

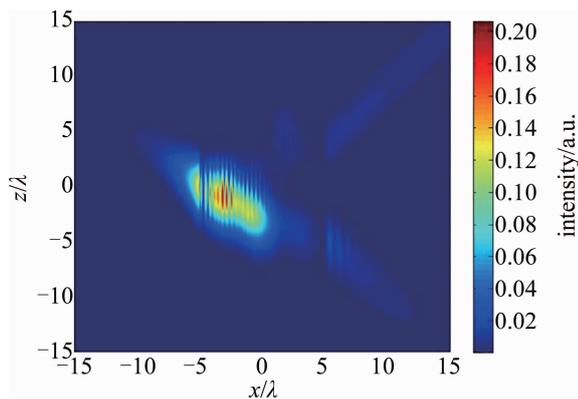


Fig. 6 The normalized internal-field and near-field of a $TEM_{10}^{(x')}$ mode Hermite-Gaussian beam through an uniaxial anisotropic cylinder

象。比较两图形,发现在相同的情况下 $TEM_{10}^{(x')}$ 模式厄米-高斯波束通过单轴各向异性圆柱时的近场强度比 $TEM_{01}^{(y')}$ 模式的强,而反射场强度弱。另一个值得注意的现象是, $TEM_{10}^{(x')}$ 模式的厄米-高斯波束在通过单轴各向异性圆柱时有一个明显的折射现象,而在 $TEM_{01}^{(y')}$ 模式厄米-高斯波束入射时则表现的不明显。

3 结论

主要基于单轴各向异性圆柱对厄米-高斯波束的散射特性进行研究。应用电磁场边界条件和投影法,精确半解析地得到了单轴各向异性圆柱对厄米-高斯波束散射特性和内场以及近场的归一化强度分布图,分析对比了两种不同的厄米高斯波束入射情形,发现波束透过圆柱后都有驻波现象。在相同的情况下 $TEM_{10}^{(x')}$ 模式厄米-高斯波束通过单轴各向异性圆柱时的近场强度比 $TEM_{01}^{(y')}$ 模式的强,而前者在通过单轴各向异性圆柱时折射现象更明显。

参考文献

- [1] ALEXOPOULOS N, PARK P K. Scattering of waves with normal amplitude distribution from cylinders[J]. IEEE Transactions on Antennas and Propagation, 1972, 20(2): 216-217.
- [2] LOCK J A. Scattering of a diagonally incident focused Gaussian beam by an infinitely long homogeneous circular cylinder [J]. Journal of the Optical Society of America, 1997, A14(3): 640-652.
- [3] GUO L X, WU Z S. Rainbow scattering by an inhomogeneous cylinder with an off-axis Gaussian beam incidence at normal[J]. International Journal of Infrared and Millimeter Waves, 2000, 21(11): 1879-1886.
- [4] ZHANG H Y, HUANG Z X, SHI Y. Internal and near-surface electromagnetic fields for a uniaxial anisotropic cylinder illuminated with a Gaussian beam[J]. Optics Express, 2013, 21(13): 15645-15653.
- [5] HUANG Z X, XU F, WANG B X, et al. Propagation of Gaussian beam through a uniaxial anisotropic slab[J]. Optics Communications, 2016, 380: 336-341.
- [6] ZHANG H Y, ZHU D, WANG M J, et al. Transmission of electromagnetic beam through a uniaxial anisotropic slab [J]. Journal of Quantitative Spectroscopy and Radiative Transfer, 2019, 224: 114-119.
- [7] CHEN Z Z, ZHANG H Y, HUANG Z X, et al. Scattering of on-axis Gaussian beam by a uniaxial anisotropic object[J]. Journal of the Optical Society of America, 2014, A31(11): 2545-2550.
- [8] GOUESBET G. Higher-order descriptions of Gaussian beams [J]. Journal of Optics (Paris), 1996, 27(1): 35-50.
- [9] KOJIMA T, YANAGIUCH Y I. Scattering of an offset two-dimensional Gaussian beam wave by a cylinder[J]. Journal of Applied Physics, 1979, 50(1): 41-46.
- [10] BARTON J P, ALEXANDER D R. Fifth-order corrected electromagnetic field components for a fundamental Gaussian beam[J]. Journal of Applied Physics, 1989, 66(7): 2800-2802.
- [11] WANG M J, ZHANG H Y, LIU G S, et al. Reflection and transmission of Gaussian beam by a uniaxial anisotropic slab[J]. Optics Express, 2014, 22(3): 3705-3711.
- [12] YE D H. Analysis and application of gauss beam characteristics [J]. Laser Technology, 2019, 43(1): 142-146 (in Chinese).
- [13] ZHU D, WU B, ZHANG H Y, et al. Transmission of arbitrary electromagnetic beam through uniaxial anisotropic cylinder[C]// 2018 Cross Strait Quad-Regional Radio Science and Wireless Technology Conference. New York, USA: IEEE, 2018:1-4.
- [14] LEI Zh, ZHANG L W, ZHANG L L, et al. Temperature field analysis and simulation of Gaussian laser irradiation focal plane detector [J]. Laser Technology, 2016, 40(4): 516-520 (in Chinese).
- [15] JIANG Q Ch, SU Y L, NIE H X, et al. Propagation characteristics of Hermite-Gaussian beam in saturated nonlinear media [J]. Laser Technology, 2018, 42(1): 141-144 (in Chinese).
- [16] LI H Y, HONORY F, WU Z S, et al. Reflection and transmission of Laguerre-Gaussian beams in a dielectric slab [J]. Journal of Quantitative Spectroscopy and Radiative Transfer, 2017, 195, 35-43.
- [17] ZHAO Q, BAI Zh Ch, ZHOU H, et al. Research of temperature and thermal stress of fused silica irradiated by Laguerre-Gaussian beam[J]. Laser Technology, 2018, 42(1): 121-126 (in Chinese).
- [18] ZAUDERER E. Complex argument Hermite-Gaussian and Laguerre-Gaussian beams [J]. Journal of the Optical Society of America, 1986, A3(4): 465-469.
- [19] DAVIS L W. Theory of electromagnetic beam[J]. Physical Review, 1979, A19(3): 1177-1179.
- [20] BARTON J P. Electromagnetic-field calculations for a sphere illuminated by a higher-order Gaussian beam. I. Internal and near-field effects[J]. Applied Optics, 1997, 36(6): 1303-1311.